Accurate small signal simulation of superconductor interconnects in SPICE

Paul Le Roux, Coenrad Fourie, Sasan Razmkhah, Pascal Febvre

Accurate small signal simulation of superconductor interconnects in SPICE

Paul le Roux, Coenrad Fourie, Sasan Razmkhah, Pascal Febvre

***Abstract*—Superconductor electronics is gaining traction as the increasing density of integration of recent and future digital circuits pushes the limits of available simulation models. Designers often make assumptions in the behavioral models of circuit elements when simulating circuits. For instance high-frequency effects have been neglected so far in the design of superconductor digital circuits, while much has been done in the past to model them. Indeed these effects had little influence on the accuracy of digital circuits simulations until recently. The increase in clock frequency, combined with longer paths between cells and higher yield requirements for large scale circuits fabrication, has led to the need of more accurate models, including in particular high frequency effects such as quasi-particle losses. To do so, this work uses a state-space model that describes the circuit under study with internal state variables and a set of first-order differential equations. We extract the state-space model while analytically enforcing the DC requirements of superconductors that are required to account for flux-trapping. The model accurately traps flux at DC, and given the model is fitted with enough poles, the high-frequency effects are also accurate relative to the reference model. The high-frequency effects have been investigated on a practical circuit: a long-distance Passive Transmission Line (PTL) designed for the high-density MIT Lincoln Labs SFQ5ee process. Results obtained in the time domain allow to observe the effects of dispersion of pulses traveling on long paths of PTLs. Indeed the energy of voltage pulses is sufficient to break Cooper pairs for the highest clock frequencies.**

***Index Terms*—Superconductor electronics, integrated circuits, passive circuits, circuit analysis**

I. Introduction

The high-frequency behavior of superconductor transmission lines has been investigated in the past for specific configurations [1]–[4], based on parameters available at the time. Smaller dimensions of contemporary superconductor circuits have led us to re-examine previous assumptions. The requirement for accurate time-domain circuit simulation models for digital circuits has been brought about by the development of complex superconductor digital circuits. Previous accurate time-domain methods utilized Fourier transforms to determine time-domain responses [2], which is impractical for large scale circuit simulations. We have recently developed a new quasi-transverse magnetic(TM) numerical method to calculate the properties of superconductor transmission lines [5]. In this work, we will fill the gap between high-frequency superconductor frequency responses and time-domain circuit models.

We assume the frequency response of PTLs is considered prior knowledge, but for specific examples we use the PTL dimensions and the response obtained from our previous work. First, the per-unit-length parameters previously calculated have to be converted into a form that relates to voltage and current. The PTL is a frequency-dependent transmission line. The electrical response can be analytically described by solving the telegraph equations. The transmission line admittance, from [6], is given by

$$\mathbf{Y}_{TL} = \begin{bmatrix} \frac{1}{Z_L \tanh(\gamma l)} & \frac{-1}{Z_L \sinh(\gamma l)} \\ \frac{-1}{Z_L \sinh(\gamma l)} & \frac{1}{Z_L \tanh(\gamma l)} \end{bmatrix}, \tag{1}$$

where Z_L is the characteristic impedance of the line, γ its propagation constant, while l is its length. Both Z_L and γ are frequency-dependent.

In this work we present superconducting vector fitting, which extends traditional vector fitting to exactly include superconductor effects. The superconductor vector fitting algorithm finds a rational polynomial to the existing superconductor response. The rational polynomial approximation, or state-space system, can be converted into an equivalent SPICE model.

II. Sanathanan Koerner Iteration

Linear time-invariant systems, such as PTLs, can be approximated using a rational polynomial function [7]. Finding a rational approximation from measured or reference information can be seen as a minimization problem, where the error between the rational model and the reference data is minimized [8], [9],

$$E(s) = H(s) - H_{fit}(s) \tag{2}$$

$$= H(s) - \frac{N(s)}{D(s)}. \tag{3}$$

The minimization problem cannot be efficiently solved with standard black box minimization techniques as small shifts in the denominator can cause large variations in the error [8], [9]. To overcome this, one can iteratively linearize the function using the previous set of poles [8]–[10],

$$E'(s) = \frac{E(s)D_n(s)}{D_{n-1}(s)} = \frac{H(s)D_n(s)}{D_{n-1}(s)} - \frac{N_n(s)}{D_{n-1}(s)}. \tag{4}$$

This iteration scheme, shown in equation (4), is known as Sanathanan-Koerner iteration [8]. A weighting term can also be added to equation (4) to assign relative importance. Each iteration is a linear least-squares problem,

$$0 \approx \frac{w(s)H(s)D_n(s)}{D_{n-1}(s)} - \frac{w(s)N_n(s)}{D_{n-1}(s)}. \tag{5}$$

The numerator coefficients are also solved in (5), but after every iteration a newer and better set of poles is available. Once the poles have been found, the numerator should be updated again with the final poles. After iteration n, the minimization of (3) corresponds to the solution of the overdetermined weighted set of equations

$$H(s) \approx \frac{w(s)N(s)}{D_n(s)} \ . \tag{6}$$

This method can be easily extended to handle vector-valued functions [9], [10].

During the pole relocation routine, we used orthogonal basis functions to speed up convergence and avoid numerical stability issues [11]. For the final fitting, we used the standard rational basis functions to reduce the size of the final state-space matrices [9].

III. Shortcoming of Vector Fitting

Vector Fitting, unfortunately, cannot directly be applied to superconductor frequency responses. We illustrate this shortcoming through an example showcasing the response of a short PTL segment. We used the cross-sectional PTL dimensions of our previous work [5], and varied the length of the PTL. We started by looking at a 10 µm-long PTL.

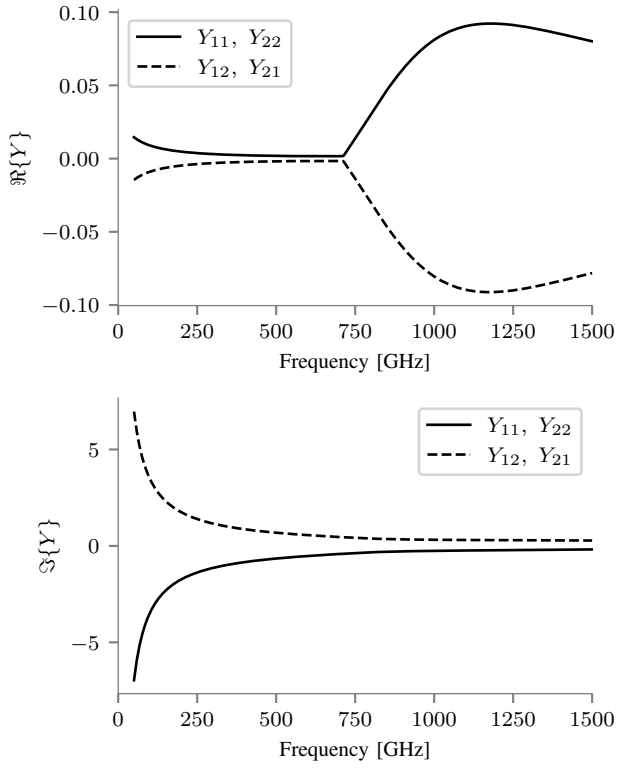

Fig. 1. Reference admittance of a 10 µm-long PTL.

Fig. 1 shows the high-frequency response of a 10 µm-long PTL. The standard Vector Fitting routine finds a rational approximation which is visually indistinguishable from the reference plot. Due to the short distance of the PTL, the attenuation is almost negligible. The short PTL can, therefore, be approximated with an inductor segment. The fitted model can be converted to an equivalent SPICE circuit and simulated [12]–[14]. The fitted model's response can then consequently be compared with the inductor model's response. We extracted an SFQ pulse from a DCSFQ circuit [15] to use as a test signal shown in Fig. 2.

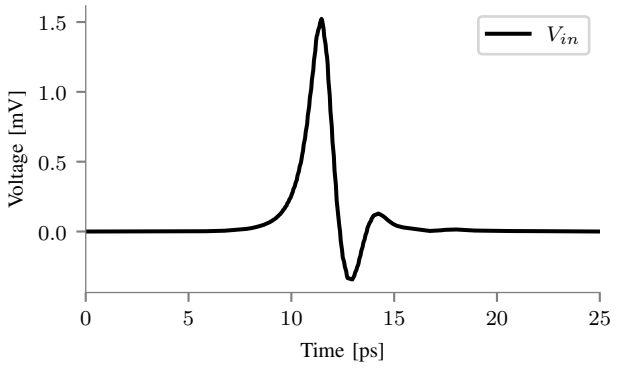

Fig. 2. SFQ pulse waveform produced by a DCSFQ cell used as a test signal.

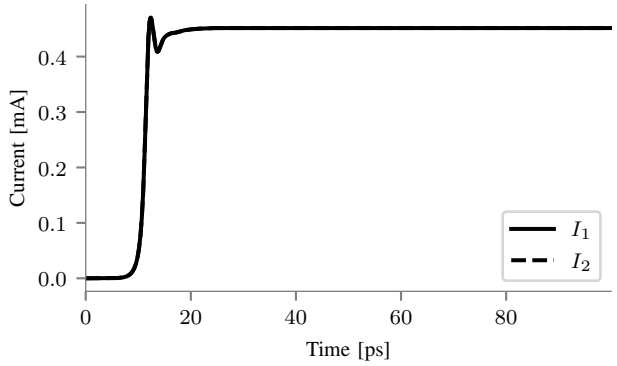

Fig. 3. Inductive response to the SFQ pulse test waveform.

The inductor's short circuit response to the SFQ pulse is shown in Fig. 3. The vector fitted model's short circuit response to the SFQ pulse is shown in Fig. 4.

The vector fitted model does not trap flux and continues to slowly decay until it reaches a zero current steady state. This is because a superconductor has zero DC resistance, which is not enforced in the vector fitted model. The standard vector fitting algorithm will therefore never exactly enforce the superconductor properties.

IV. Superconductor Vector Fitting

The inaccuracies of fitting a function with a pole outside the fitting range are already mentioned in [9]. We observe precisely the error that is observed in [9]. The fit is accurate

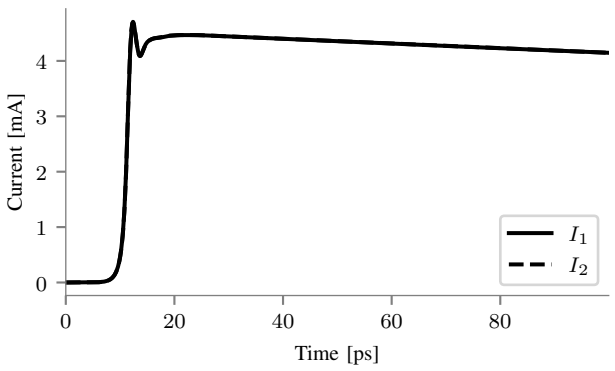

Fig. 4. Vector Fitted response to the SFQ pulse test waveform.

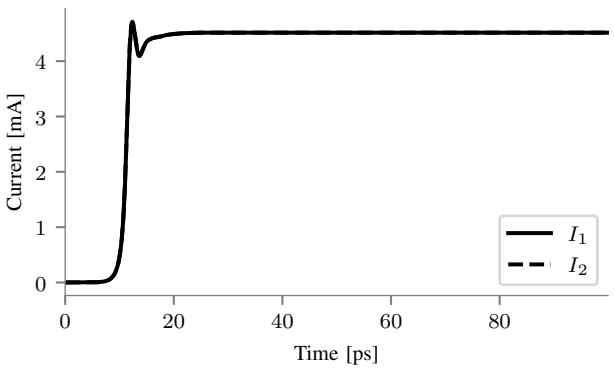

Fig. 5. Superconductor Vector Fitted response to the SFQ test waveform

in the fitting range with large errors outside of the fitting range around the external pole.

It would be tempting to fit the impedance with $w = 0$ included in the fitting range, but the system of equations is enforced in a least-squares sense. The impedance would not be exactly 0, which is the requirement for the model to behave like a superconductor. For superconductor vector fitting the superconducting effect has to be exactly enforced.

Given an n-port system where port i is connected to the ground with a superconductor then

$$\lim_{\omega\to 0} Y_{ii}(\omega) = \lim_{\omega\to 0} \frac{1}{j\omega L_{ii}} = -j\infty, \tag{7}$$

where L_{ii} is the equivalent inductance to ground of the ith port. The ports of the admittance are considered shorted, and (7) is also true if it is connected with a superconductor to another port.

Given an n-port system where port i is connected with a superconductor to ports j_x then

$$\lim_{\omega\to 0} Y_{ij}(\omega) = \lim_{\omega\to 0} \frac{-1}{j\omega L_{ij}} = j\infty. \tag{8}$$

We can therefore subtract the DC inductance response from the superconductor to get a response which can then be fitted using standard vector fitting techniques. This is analogous to modelling a black box system with a known inductor system in parallel with another black box system.

We want to reformulate the weighted fitting function with a known parallel system. We assume H_{fit} is the summation of an unknown system, $H^{'}_{fit}$ and a known system, H_{prior}. By subtracting the known system multiplied by the weight function from (9) we manipulate (9) into

$$wH_{fit} \approx wH \tag{9}$$

$$wH^{'}_{fit} \approx w(H - H_{prior}). \tag{10}$$

The final state-space system can be constructed by adding the two in parallel. The state-space system is given by

$$s\mathbf{X}(s) = \begin{bmatrix}\mathbf{A}_{prior} & \mathbf{0}\\ \mathbf{0} & \mathbf{A}\end{bmatrix}\mathbf{X}(s) + \begin{bmatrix}\mathbf{B}_{prior}\\ \mathbf{B}\end{bmatrix}\mathbf{U}(s), \text{ and} \tag{11}$$

$$\mathbf{Y}(s) = \begin{bmatrix}\mathbf{C}_{prior} & \mathbf{C}\end{bmatrix}\mathbf{X}(s) + (\mathbf{D}_{prior} + \mathbf{D})\mathbf{U}(s). \tag{12}$$

We can now fit superconductor responses and exactly enforce the required DC conditions. Using the newly developed superconductor vector fitting we again fit the $10\,\mu\mathrm{m}$ long PTL and excite it using our test signal.

Fig. 5 shows that the model correctly traps flux and has zero DC-losses. We now move on to a more complex $1\,\mathrm{mm}$-long PTL example.

Fig. 6 shows the reference admittance of the $1\,\mathrm{mm}$-long PTL. The superconductor vector fitting algorithm finds a fit which is visually indistinguishable from the curve of Fig. 1.

V. Modality

For the model to be accurate under all loading conditions, the model's eigenvalues have to be accurate [16]. To investigate the model's modal accuracy, we calculate its inverse to get the impedance and compare it to the expected impedance. Fig. 7 and Fig. 8 show respectively the reference impedance of the $1\,\mathrm{mm}$-long PTL, and the impedance obtained by the superconductor vector fitted method. One sees that this second impedance deviates significantly from the expected curve, as displayed in Fig. 9 with the eigenvalue error of the $1\,\mathrm{mm}$ long PTL model. This extreme error instils doubt into any time-domain simulation results and has to be addressed.

Existing modal vector fitting techniques [16], [17], cannot be applied verbatim to superconductor vector fitting. Since the PTL is a reciprocal, and symmetrical 2-port system, we can use the real transform method [16].

$$\mathbf{T}_2 = \begin{bmatrix}-\frac{1}{\sqrt{2}} & \frac{1}{\sqrt{2}}\\ \frac{1}{\sqrt{2}} & \frac{1}{\sqrt{2}}\end{bmatrix} \tag{13}$$

The transform matrix, $\mathbf{T}_2$, is unitary and symmetric. The transformed admittance of the transmission line is then

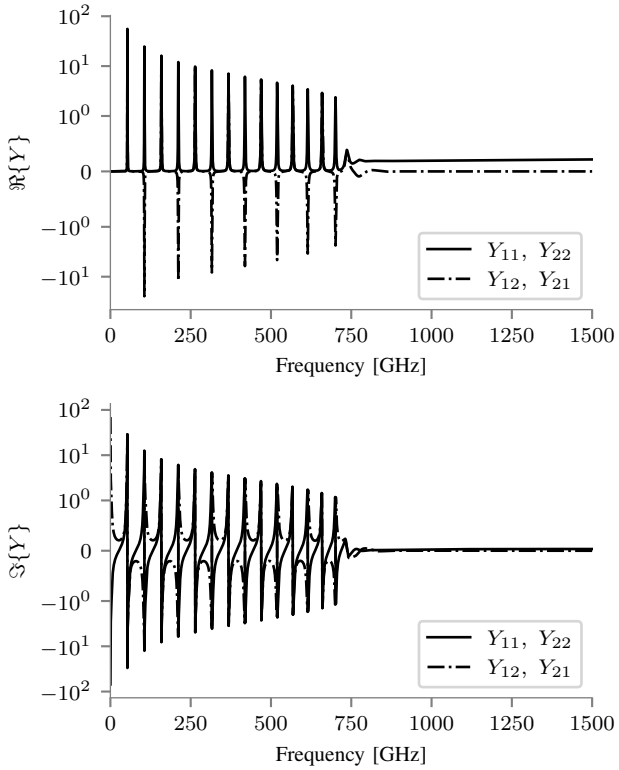

Fig. 6. Reference admittance of a 1 mm-long PTL

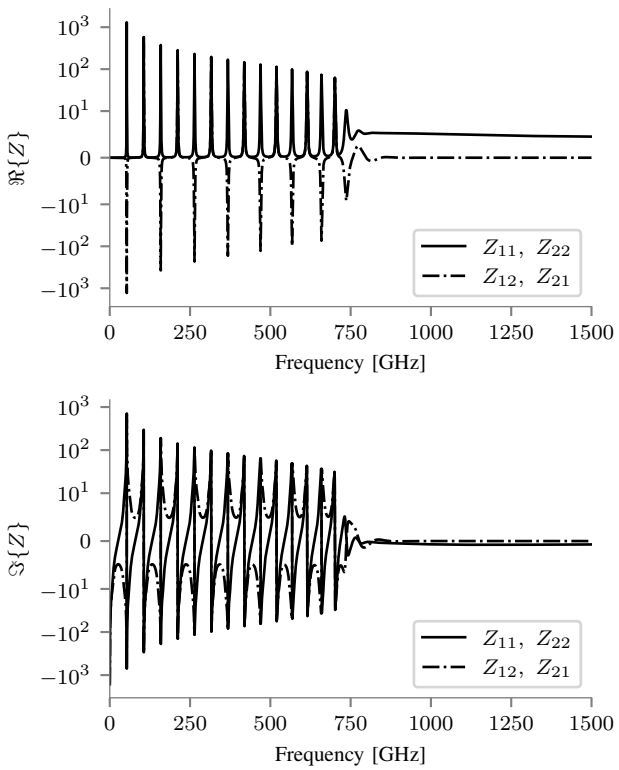

Fig. 7. Reference impedance of a 1 mm-long PTL

$$\mathbf{T}_2 \cdot \mathbf{Y}_{TL} \cdot \mathbf{T}_2 = \begin{bmatrix} \frac{1}{Z_L}\coth(\frac{\gamma l}{2}) & 0 \\ 0 & \frac{1}{Z_L}\tanh(\frac{\gamma l}{2}) \end{bmatrix}, \quad (14)$$

where the diagonal entries are the eigenvalues of the response. To enforce the superconductor response we, again, subtract the superconductor response,

$$\mathbf{T}_2 \cdot \mathbf{Y}_{TL} \cdot \mathbf{T}_2 = \begin{bmatrix} \frac{1}{Z_L}\coth(\frac{\gamma l}{2}) - \frac{2}{Z_L \gamma l} & 0 \\ 0 & \frac{1}{Z_L}\tanh(\frac{\gamma l}{2}) \end{bmatrix}. \quad (15)$$

To enforce modal accuracy, the eigenvalues should be weighted inversely proportional to their magnitude before the superconductor effect was subtracted. Looking at the second eigenvalue, we see that

$$\lim_{\omega \to 0} \left\{ \frac{1}{Z_L}\tanh(\frac{\gamma l}{2}) \right\} = 0. \quad (16)$$

This implies that the weight function should be infinite at DC. Alternatively stated, the second eigenvalue should be exactly zero. Conveniently, the first eigenvalue is also zero after the superconductor effect has been subtracted.

$$\lim_{\omega \to 0} \left\{ \frac{1}{Z_L}\coth(\frac{\gamma l}{2}) - \frac{2}{Z_L \gamma l} \right\} = 0 \quad (17)$$

We now want to reformulate the weighted fitting problem to enforce zeros at the origin. We assume H_{fit} has a zero at the origin and can be defined as $H_{fit} = sH_{fit}^{'}$. By multiplying the right hand side of (9) with $1 = \frac{s}{s}$ we manipulate (9) into

$$(sw)H_{fit}^{'} \approx (sw)\frac{H}{s}. \quad (18)$$

Equation (18) corresponds to fitting the integrated system. The integrated system can then be differentiated to get the final system.

We, therefore, need to find the state space representation of a differentiated system. We start from the transfer function to derive the state space representation of a differentiated system.

$$\begin{aligned} \mathbf{H}(s) &= \mathbf{C}(s\mathbf{I} - \mathbf{A})\mathbf{B} + \mathbf{D} \\ \mathbf{h}(t) &= \mathbf{C}e^{\mathbf{A}t}\mathbf{B} + \mathbf{D}\delta(t) \\ \frac{d}{dt}\mathbf{h}(t) &= \mathbf{C}\mathbf{A}e^{\mathbf{A}t}\mathbf{B} + \frac{d}{dt}\mathbf{D}\delta(t) \\ s\mathbf{H}(s) - \mathbf{h}(0^+) &= \mathbf{C}\mathbf{A}(s\mathbf{I} - \mathbf{A})\mathbf{B} + s\mathbf{D} - \mathbf{D}\delta(0^+) \\ s\mathbf{H}(s) &= \mathbf{C}\mathbf{A}(s\mathbf{I} - \mathbf{A})\mathbf{B} + \mathbf{C}\mathbf{B} + s\mathbf{D} \end{aligned} \quad (19)$$

We now have everything we need to implement a program that can determine a PTL model while enforcing modal accuracy. Fitting the PTL using modal superconductor vector fitting we get a model which is, again, visually indistinguishable from the reference admittance. The model's impedance is also visually indistinguishable from the reference impedance.

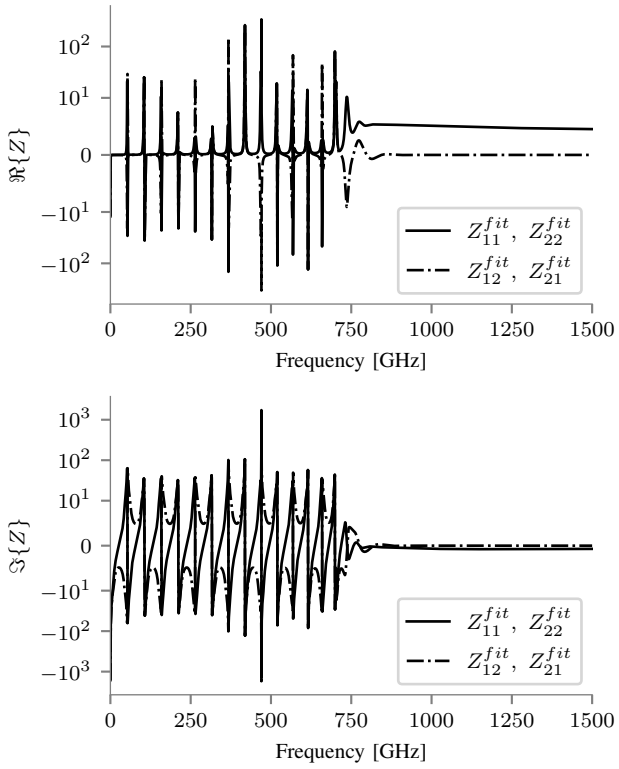

Fig. 8. The impedance of the 1 mm-long PTL Superconductor Vector Fitted model.

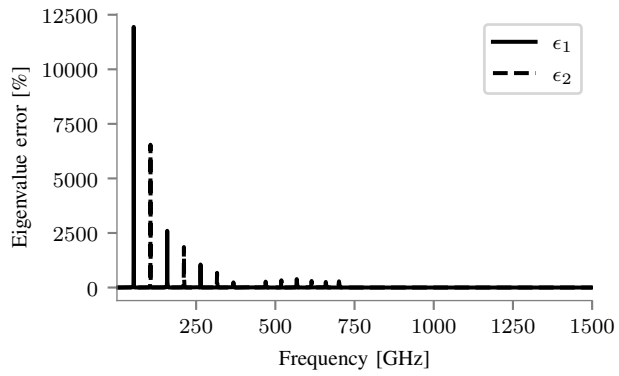

Fig. 9. Eigenvalue error of the 1 mm-long PTL Superconductor Vector Fitted model

Fig. 10 shows the eigenvalue error of the Modal Superconductor Vector Fitted PTL model. From the error plot, we can see that most of the error sits around the gap frequency. This is due to the discontinuous derivative at the gap frequency, which cannot be exactly enforced by any rational polynomial model. Fortunately, the error is still small, and SFQ pulses have little energy in the bandwidth around the gap frequency.

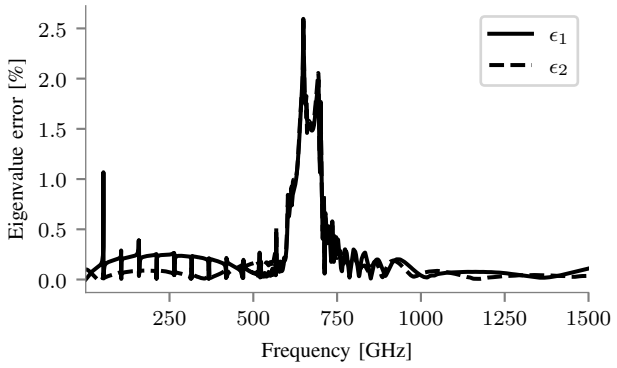

Fig. 10. Eigenvalue error of the 1 mm-long PTL Superconductor Modal Vector Fitted PTL model

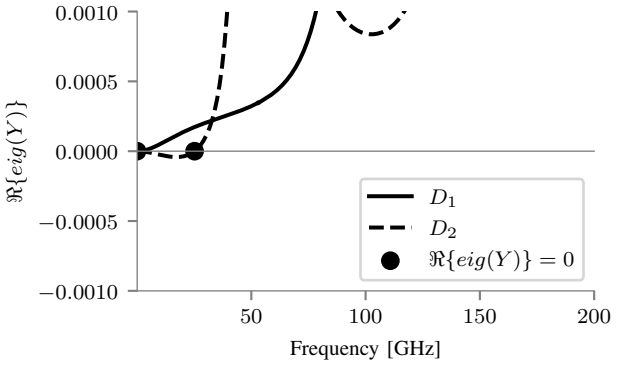

Fig. 11. Conductance eigenvalues of the 1 mm-long PTL Superconductor Modal Vector Fitted model.

VI. Passivity

For a time-domain model to be stable, it must be passive [18]. Non-passive circuits can cause result in runaway amplification of numerical error, which prevents any useful simulation. We must, therefore, ensure our model is passive in addition to the above accuracy requirements.

For a system to be passive, the eigenvalues of the conductance should be positive.

$$eig(\Re\{\mathbf{Y}\}) >= \mathbf{0} \tag{20}$$

Fig. 11 shows the conductance values of superconductor modal fitted PTL. It is clear that our model is currently not passive and generates energy in the low GHz range.

Fortunately, the standard passivity enforcement techniques that are used in standard vector fitting can be directly applied to the modal superconductor vector fitting algorithm. Many methods exist for passivity enforcement [18]–[21]. Due to its effectiveness, we will use residue perturbation to passivate the PTL model. When performing the final fit, linearized constraints are added to ensure that the eigenvalues of the conductance are positive [18].

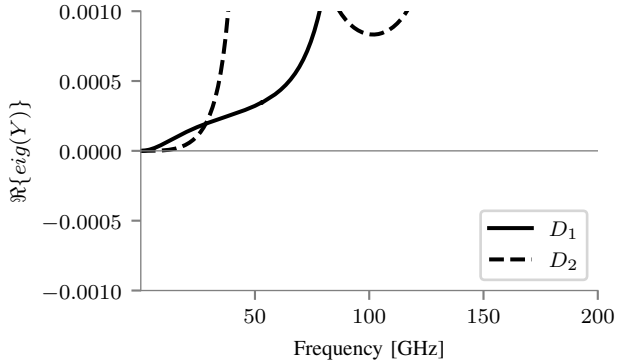

Fig. 12. Conductance eigenvalues of the 1 mm-long PTL Passivated Superconductor Modal Vector Fitted model.

We used the half-size singularity test matrix [22] to determine the frequency bands in which the passivity condition is violated. We added constraining equations in the centre of each violation band. The resulting constrained least-squares problem is a special case of the quadratic programming problem. We used cvxopt [23] to solve the quadratic programming equivalent of the constrained least-squares problem. If the model still has passivity violations, the residue is perturbated again.

Fig. 12 shows the conductance values of the passivated superconductor modal fitted PTL. The model no longer has any passivity violations.

VII. Results

With an accurate time-domain model, we can investigate how long-distance PTLs shape SFQ pulses.

Fig. 13 shows the SFQ pulse as it travels on a PTL. We used JoSIM [24] for the simulation. The pulse spreads and develops an oscillating tail. It deviates significantly from an ideal transmission line response in which the waveform remains unchanged. This is in line with results obtained using the Fourier transform [2].

We can also see that the SFQ pulse remains quantized. Even though the SFQ pulse remains quantized, it does dissipate energy as it moves along the line. This dissipation in energy will directly influence the ability of a receiving junction to trigger.

VIII. Conclusion

We have demonstrated Superconductor Vector Fitting as an extension to standard Vector Fitting. With the Superconductor Vector Fitting algorithm, we can find an accurate, rational approximation of a PTL from the PTL's frequency response. The rational approximation can then easily converted into a SPICE subcircuit. In addition, we have shown how to enforce modal accuracy in the superconductor case, and that standard passivization algorithms are applicable. The resulting SPICE subcircuit was used to investigate the effect that the PTL has on an SFQ pulse. The pulse was shown to remain quantized, but lose energy and spread out as it travels along on a PTL.

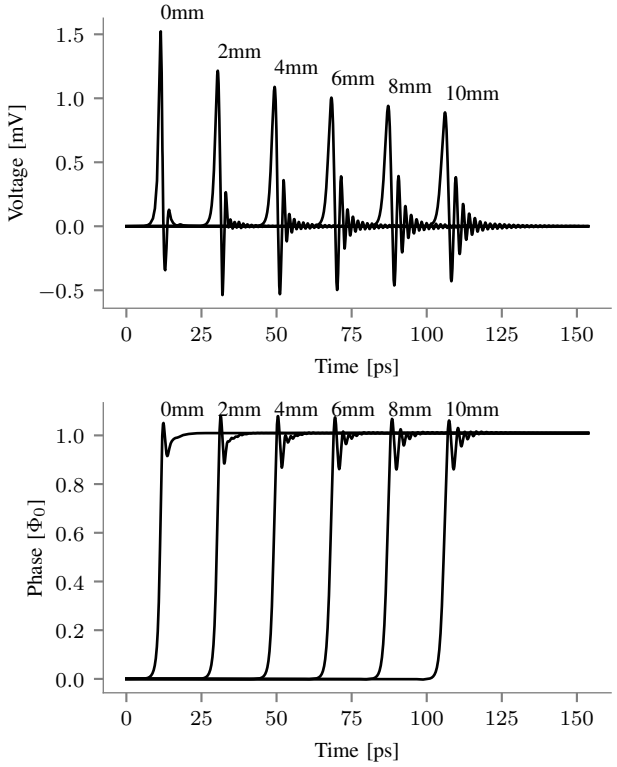

Fig. 13. Voltage and phase of a travelling SFQ pulse along the PTL, simulated with the Passivated Superconductor Modal Vector model

IX. Acknowledgments

The research is based upon work supported by the Office of the Director of National Intelligence (ODNI), Intelligence Advanced Research Projects Activity (IARPA), via the U.S. Army Research Office grant W911NF-17-1-0120.

References

[1] P. V. Mason and R. W. Gould, "Slow-Wave Structures Utilizing Superconducting Thin-Film Transmission Lines," *Journal of Applied Physics*, vol. 40, no. 5, pp. 2039–2051, Apr 1969. [Online]. Available: http://aip.scitation.org/doi/10.1063/1.1657907

[2] J. Whitaker, R. Sobolewski, D. Dykaar, T. Hsiang, and G. Mourou, "Propagation model for ultrafast signals on superconducting dispersive striplines," *IEEE Transactions on Microwave Theory and Techniques*, vol. 36, no. 2, pp. 277–285, 1988. [Online]. Available: http://ieeexplore.ieee.org/document/3516/

[3] J. Chwalek, D. Dykaar, J. Whitaker, R. Sobolewski, S. Gupta, T. Hsiang, and G. Mourou, "Ultrafast response of superconducting transmission lines," *IEEE Transactions on Magnetics*, vol. 25, no. 2, pp. 814–817, Mar 1989. [Online]. Available: http://ieeexplore.ieee.org/document/92410/

[4] J. Tao, A. Roussy, P. Febvre, J. Villegier, and N. Hadacek, "Fullwave frequency dependent inductance estimation for rsfq applications in nbn multilayer technology," in *2000 30th European Microwave Conference*. IEEE, 2000, pp. 1–4.

[5] P. le Roux, K. Jackman, J. A. Delport, and C. J. Fourie, "Modeling of Superconducting Passive Transmission Lines," *IEEE Trans. on Appl. Supercond.*, vol. 29, no. 5, pp. 1–5, Aug 2019.

[6] S. Jahn, M. Margraf, V. Habchi, and R. Jacob, "QUCS Online Technical Manual." [Online]. Available: http://qucs.sourceforge.net/tech/technical.html

[7] E. C. Levy, "Complex-curve fitting," *IRE Transactions on Automatic Control*, vol. AC-4, no. 1, pp. 37–43, 1959. [Online]. Available: http://ieeexplore.ieee.org/document/6429401/

[8] C. Sanathanan and J. Koerner, "Transfer function synthesis as a ratio of two complex polynomials," *IEEE Transactions on Automatic Control*, vol. 8, no. 1, pp. 56–58, Jan 1963. [Online]. Available: http://ieeexplore.ieee.org/document/1105517/

[9] B. Gustavsen and A. Semlyen, "Rational approximation of frequency domain responses by vector fitting," *IEEE Transactions on Power Delivery*, vol. 14, no. 3, pp. 1052–1061, Jul 1999. [Online]. Available: http://ieeexplore.ieee.org/document/772353/

[10] W. Hendrickx and T. Dhaene, "A Discussion of "Rational Approximation of Frequency Domain Responses by Vector Fitting"," *IEEE Transactions on Power Systems*, vol. 21, no. 1, pp. 441–443, Feb 2006. [Online]. Available: http://ieeexplore.ieee.org/document/1583747/

[11] D. Deschrijver, B. Haegeman, and T. Dhaene, "Orthonormal Vector Fitting: A Robust Macromodeling Tool for Rational Approximation of Frequency Domain Responses," *IEEE Transactions on Advanced Packaging*, vol. 30, no. 2, pp. 216–225, May 2007. [Online]. Available: http://ieeexplore.ieee.org/document/4214901/

[12] J. Hewlett and B. Wilamowski, "SPICE as a Fast and Stable Tool for Simulating a Wide Range of Dynamic Systems," *International Journal of Engineering Education*, vol. 27, pp. 217–224, 2011.

[13] W. R. Zimmerman, "Time domain solutions to partial differential equations using spice," *IEEE Transactions on Education*, vol. 39, no. 4, pp. 563–573, 1996.

[14] G. Antonini, "Spice equivalent circuits of frequency-domain responses," *IEEE Transactions on Electromagnetic Compatibility*, vol. 45, no. 3, pp. 502–512, 2003.

[15] Lieze Schindler, "RSFQlib." [Online]. Available: https://github.com/sunmagnetics/RSFQlib

[16] B. Gustavsen and C. Heitz, "Modal Vector Fitting: A Tool For Generating Rational Models of High Accuracy With Arbitrary Terminal Conditions," *IEEE Transactions on Advanced Packaging*, vol. 31, no. 4, pp. 664–672, Nov 2008. [Online]. Available: http://ieeexplore.ieee.org/document/4601493/

[17] B. Gustavsen and C. Heitz, "Fast Realization of the Modal Vector Fitting Method for Rational Modeling With Accurate Representation of Small Eigenvalues," *IEEE Transactions on Power Delivery*, vol. 24, no. 3, pp. 1396–1405, Jul 2009. [Online]. Available: http://ieeexplore.ieee.org/document/4895724/

[18] B. Gustavsen and A. Semlyen, "Enforcing passivity for admittance matrices approximated by rational functions," *IEEE Transactions on Power Systems*, vol. 16, no. 1, pp. 97–104, 2001. [Online]. Available: http://ieeexplore.ieee.org/document/910786/

[19] B. Gustavsen, "Passivity Enforcement of Rational Models via Modal Perturbation," *IEEE Transactions on Power Delivery*, vol. 23, no. 2, pp. 768–775, Apr 2008. [Online]. Available: http://ieeexplore.ieee.org/document/4476471/

[20] B. Gustavsen, "Fast passivity enforcement of rational macromodels by perturbation of residue matrix eigenvalues," in *2007 IEEE Workshop on Signal Propagation on Interconnects*. IEEE, May 2007, pp. 71–74. [Online]. Available: http://ieeexplore.ieee.org/document/4512213/

[21] S. Grivet-Talocia, "Passivity Enforcement via Perturbation of Hamiltonian Matrices," *IEEE Transactions on Circuits and Systems I: Regular Papers*, vol. 51, no. 9, pp. 1755–1769, Sep 2004. [Online]. Available: http://ieeexplore.ieee.org/document/1333225/

[22] A. Semlyen and B. Gustavsen, "A Half-Size Singularity Test Matrix for Fast and Reliable Passivity Assessment of Rational Models," *IEEE Transactions on Power Delivery*, vol. 24, no. 1, pp. 345–351, Jan 2009. [Online]. Available: http://ieeexplore.ieee.org/document/4512041/

[23] M. Andersen, J. Dahl, and L. Vandenberghe, "CVXOPT." [Online]. Available: https://cvxopt.org/index.html

[24] J. A. Delport, K. Jackman, P. Le Roux, and C. J. Fourie, "Josim—superconductor spice simulator," *IEEE Trans. on Appl. Supercond.*, vol. 29, no. 5, pp. 1–5, 2019.